Leptospiral lipopolysaccharide dampens inflammation through upregulation of autophagy adaptor p62 and NRF2 signaling in macrophages

Delphine Bonhomme [a], Ignacio Santecchia [a], Pedro Escoll [b], Stylianos Papadopoulos [a], Frédérique Vernel-Pauillac [a], Ivo G. Boneca [a] & Catherine Werts [a*]

[a] Institut Pasteur, Université Paris Cité, CNRS UMR6047, INSERM U1306, Unité de Biologie et Génétique de la Paroi Bactérienne, Paris, France

[b] Institut Pasteur, Université Paris Cité, CNRS UMR6047, Unité Biologie des Bactéries Intracellulaires, Paris, France

RUNNING HEAD (54 characters): Leptospires dampen inflammation through p62-NRF2 activation

*Corresponding Author: Catherine Werts

Institut Pasteur

28 rue du Dr Roux

Unité BGPB, Microbiology Dpt

Paris 75015 FRANCE

Tel: +33(0)609537030

E-mail: cwerts@pasteur.fr

NUMBER OF TABLES : 2

NUMBER OF FIGURES : 5

WORD COUNT (Introduction- Materials&Methods-Results-Discussion- Acknowledgments): 4705

KEY WORDS: *Leptospira*, LPS, TLRs, Autophagy adapter p62, NRF2

ABSTRACT (247 words)

Leptospira interrogans are pathogenic bacteria responsible for leptospirosis, a worldwide zoonosis. All vertebrates can be infected, and some species like humans are susceptible to the disease whereas rodents such as mice are resistant and become asymptomatic renal carriers. Leptospires are stealth bacteria that are known to escape several immune recognition pathways and resist killing mechanisms. We recently published that leptospires may survive intracellularly and exit macrophages, in part by escaping xenophagy, a pathogen-targeting form of autophagy. Interestingly, autophagy is one of the antimicrobial mechanisms often highjacked by bacteria to evade the host immune response. In this study we therefore explored whether leptospires subvert the key molecular players of autophagy to facilitate the infection. We showed in macrophages that leptospires triggered a specific accumulation of autophagy-adaptor p62 in puncta-like structures, without major alteration of autophagy flux. Unlike active bacterial mechanisms described to date, we demonstrated that leptospires trigger p62 accumulation using a passive mechanism of LPS signaling via TLR4/TLR2. p62 is a central pleiotropic protein, not only involved in autophagy, but also mediating cell stress and death, *via* the translocation of transcription factors. We demonstrated that *Leptospira*-driven accumulation of p62 induced the translocation of transcription factor NRF2. However, NRF2 translocation upon *Leptospira* infection did not result as expected in antioxydant response, but dampened the production of inflammatory mediators such as iNOS/NO, TNF and IL6. Overall, these findings highlight a novel passive bacterial mechanism linked to p62/NRF2 signaling that decreases inflammation and contributes to the stealthiness of leptospires.

INTRODUCTION

Leptospira interrogans are spirochete bacteria and the causative agent of leptospirosis, a neglected worldwide zoonosis whose global impact on human health is increased due to climate change, and causes around 60 000 deaths *per* year worldwide (1). Although all vertebrates can be infected by leptospires, they do not all present the same symptoms and susceptibility to the disease (2). Humans, as sensitive hosts, may suffer from acute leptospirosis ranging from flu-like symptoms to multi-organ

55 failure in 5-10% cases (1). On the other hand, rodents such as mice and rats are resistant to acute illness
56 and become chronically colonized upon infection (3). Leptospires establish a stable colonization in the
57 proximal tubules in the kidneys, that leads to their excretion in the urine throughout the life of the animal,
58 contributing to the spread of the zoonosis (3, 4).

59 Upon infection, the host immune defenses rely on humoral and cellular components, such as the
60 complement system, immunoglobulins, and patrolling phagocytes. Activation of immune cells such as
61 macrophages is mediated by the sensing of microbial associated molecular patterns (MAMPs) by pattern
62 recognition receptors (PRRs). Leptospires are agonists of TLR2, through their numerous lipoproteins
63 (5, 6), and activate the NLRP3 inflammasome (7). However, they are remarkable as stealth pathogens
64 that escape recognition by NOD receptors (8) and by TLR5 (9) through unique mechanisms.
65 Furthermore, the leptospiral lipopolysaccharide (LPS), a central virulence factor (10), possesses
66 structural peculiarities (11) that do not activate human TLR4 (12), whereas they partially activate murine
67 TLR4 (13). In addition to escaping PRR recognition, leptospires also escape some phagocytic functions.
68 Although leptospires are mostly extracellular bacteria, we previously reported that they can be found
69 within macrophages without intracellular replication (14), and are neither targeted by phagocytosis nor
70 classical microbicidal compounds (14). We further excluded that intracellular leptospires could be
71 targeted by xenophagy (14), a specific form of autophagy promoting the degradation of intracellular
72 pathogens (15-17).

73 Interestingly, among the numerous proteins involved in autophagy, many have pleiotropic roles
74 that are not restricted to autophagic-degradation and are at the crossroads between autophagy, cell death,
75 cellular stress and inflammation. For instance, autophagy adaptors p62 and NDP52, which traditionally
76 bridge the cargo and autophagosome for specific degradation, have been associated with many
77 xenophagy-independent inflammatory modulations (18, 19). Both p62 and NDP52 have been shown to
78 mediate nuclear translocation of transcription factors NFκB and NRF2, which are involved in
79 inflammation and cellular stress, respectively (18, 20).

80 In this study, we focused our investigations on autophagy adaptors and unexpectedly found in
81 macrophages infected with leptospires a role of their LPS in dampening of inflammation through a
82 modulation of the p62/ NRF2 axis.

83

84 **MATERIALS AND METHODS**

85 ***Leptospira interrogans* cultures.** *Leptospira interrogans* used (Manilae strain L495, Copenhageni
86 strain Fiocruz L1-130, Icterohaemorragiae strain Verdun) and *Leptospira biflexa* (Patoc strain Patoc I)
87 were grown in Ellinghausen-McCullough-Johnson-Harris (EMJH) medium at 28°C without agitation
88 and diluted weekly (twice a week for *L. biflexa*) to obtain exponential cultures. For infection, cultures
89 were centrifuged (3250 g, 25 min), resuspended in PBS (Lonza), and enumerated in Petroff-Hauser
90 chamber. Inactivated leptospires ("heat-killed") were heated at 56 °C for 30 min with mild agitation.
91 For fluorescent labelling, 10 mL of exponential culture was centrifuged (3250 g, 25 min) and the pellet
92 was resuspended in the same volume of PBS (Lonza) with addition of 10 µM CFSE (Sigma) for 30 min,
93 followed by one wash in PBS before counting and infection.

94 **Mice experiments.** Adults male and female C57/BL6 mice (Janvier Labs, Le Genest-Saint-Isle, France)
95 were injected *via* intraperitoneal route with 1 x10^8 heat-killed leptospires/mouse in PBS. Next, 4h post-
96 infection mice were euthanized, and peritoneal content was recovered as previously described (21).
97 Peritoneal cells were plated at 1 x10^6 cells/mL and were let to adhere for 1h before fixation and
98 immunofluorescence staining.

99 **Cell culture.** BMDMs were obtained and derived from adults male and female mice of either C57BL/6
100 WT (Janvier Labs, Le Genest-Saint-Isle, France) or TLR2$^{-/-}$ TLR4$^{-/-}$ (from Institut Pasteur) as described
101 before (13). BMDMs were seeded in plates (TPP) the day before infection at a concentration of 0.8 x10^6
102 cells/mL, in antibiotic-free complete RPMI (RPMIc) (containing glutamine (Lonza), supplemented with
103 10 % v/v heat-inactivated fetal calf serum (HI-FCS, Gibco), 1 mM non-essential amino acids (NEA,
104 Gibco) and 1 mM sodium pyruvate (NaPy, Gibco)).

105 RAW264.7 murine macrophage-like cell line was cultured in antibiotic-free RPMIc.
106 RAW-mLC3-DiFluo (Invivogen) autophagy reporter cells (transfected with LC3-GFP-RFD) were
107 cultured with 100 µg/mL zeocin (Invivogen). Cells were seeded in plates (TPP) the day before infection
108 at a concentration of 0.3 x10^6 cells/mL, in antibiotic-free RPMIc.

109 Human THP-1 monocyte-like cell line, stably transfected with CD14 (THP1-CD14), was cultured in
110 RPMIc and seeded at 1 x10^6 cells/mL.

111 All cell cultures were tested negative for *Mycoplasma* contamination, and all cell cultures used for
112 experiments were maintained under 80 % confluence in order to prevent autophagic stress.

113 Cell starvation was induced in EBSS media (Gibco) after 2 washes. Autophagy blockage was induced
114 with 100 nM bafilomycin A1 (BafA1, Sigma-Aldrich) 4h before cell collection. Inflammasome
115 inhibition was triggered using 25 µM glibenclamide (Thermo Fisher) 30 min before infection. Finally,
116 stimulations by leptospiral LPS were performed with 1 µg/mL of LPS of *L. interrogans* L495 extracted
117 from the phenolic phase of the hot water/phenol extraction protocol, as we recently reviewed (22).

118 **Immunofluorescence and High Content (HC) automated microscopy.** Cells were seeded and
119 infected on cover glass (18 mm diameter, # 1.5 thickness, Electron Microscopy Science) and were fixed
120 in 4 % v/v *para*-formaldehyde for 10 min, followed by three washes with PBS. Blocking was 1h in PBS
121 + 5% w/v bovine serum albumin (BSA) and 2.5 µg/mL anti-CD16-CD32 (FcBlock, Thermo Fisher).
122 Primary antibodies (**Table 1**) or isotypes were incubated overnight at 4 °C in PBS + 1% w/v BSA,
123 0.05% w/v saponin. Cells were then washed three times with PBS + 0.05% w/v saponin and labeled for
124 1h with secondary antibodies when necessary (**Table 1**) and 1µg/mL DAPI in PBS + 1% w/v BSA,
125 0.05% w/v saponin. For NRF2 nuclear staining, permeabilization was performed in PBS + 1% w/v BSA,
126 0.5% v/v Triton X-100 for 10 min prior to blocking. Image acquisition was performed on Leica SP5
127 confocal microscope (63x - 1.4 NA, oil immersion). Default settings were used and both UV and argon
128 lasers were used at power between 10-30 %.

129 For HC automated microscopy, cells were seeded in dark, transparent bottom 96-well plates
130 (Greiner, µClear) at 0.1 x10^6 cells/mL. Cells were stained as described, except for RAW-mLC3-DiFluo

131 that were fixed 10 min in cold ethanol/acetone (1:1). Imaging was performed on Opera Phenix (Perkin
132 Elmer) using confocal settings and 63X water-immersion objective (NA 1.15). Light source was kept at
133 20 to 50% power and exposure time was set to obtain intensities 1000-5000. Automated acquisition
134 allowed analysis of 500-1000 cells/well in technical triplicates for each experiment. Automated image
135 analysis workflow and puncta quantification was performed using Columbus image data storage and
136 analysis system (PerkinElmer), with the following steps: *(i)* import data; *(ii)* find nuclei with DAPI
137 signal; *(iii)* find cytoplasm using target protein signal (p62 / NRF2 / F4/80); *(iv)* select cell population
138 of interest if relevant (F4/80$^+$ peritoneal cells), *(v)* find spots if relevant (p62); *(vi)* formulate classical
139 outputs: number of p62 puncta, NRF2 intensity in nucleus/cytoplasm; *(vii)* formulate calculated
140 outputs: %p62 positive cells, NRF2 ratio, %NRF2 positive cells*; (viii)* save script and run batch analysis
141 and *(ix)* export data.

142 **SDS-PAGE and Western blot**. For Western blot, cells were scrapped and centrifuged (400 g, 10 min).
143 Pellets were resuspended in 50 µL of ice-cold RIPA lysis buffer supplemented with 1x complete Mini,
144 EDTA-free proteases inhibition cocktail (Roche). Cells were lysed on ice for 15 min followed by
145 centrifugation (12000 g, 40 min, 4 °C). Soluble proteins were recovered in the supernatant and dosed
146 using the Bradford assay and the samples were denatured in Laemli buffer (99 °C, 10 min). SDS-PAGE
147 was performed at 100 V on 4-15% gradient acrylamide Stain-free gels in Tris-Glycine-SDS buffer
148 (BioRad), with 5-10 µg of protein. Total proteins were visualized as internal control using stain free
149 reagent in ChemiDoc (BioRad) with a 5 min exposition time and then transferred on 0.22 µm PVDF
150 membrane (BioRad) using Mixed MW fast transfer of 1 miniGel (BioRad). Membrane was blocked 1h
151 in TBS with 0,05% v/v Tween 20 (TBS-T) + 5% w/v BSA. The membrane was probed overnight at
152 4 °C with primary antibodies (**Table 1**) in TBS-T + 5% w/v BSA. After three washes, membrane was
153 incubated 1h with secondary anti-rabbit IgG HRP-linked (**Table 1**) in TBS-T + 5% w/v BSA. After
154 three washes, blots were revealed using the Clarity reagent (BioRad) with automatic exposure time.

155 **Small interfering RNA transfection.** For siRNA transfection, cells were seeded at confluence of
156 0.1 x10^6 cells/mL the day before transfection. Transfection was performed using Lipofectamine
157 siRNA Max reagent (ThermoFisher) OptiMEM media (Gibco) and according to the manufacturer's

158 instructions. The final concentration of commercial predesigned siRNA targeting *p62* and *nrf2*
159 (FlexiTube, Qiagen) was 80 nM and the corresponding scramble siRNA (all start negative, Qiagen) was
160 used as control. The siRNA preparations in lipofectamine were incubated at room temperature for
161 25 min before delicate transfection of the cells in OptiMEM. After 8 hours, the same volume of RPMIc
162 was added for overnight incubation. Infection was performed the next day in RPMIc after complete
163 media removal.

164 **ELISA and Griess reaction**. Fresh cell culture supernatants were used 24h post-infection for dosage
165 of nitric oxide (NO) by the Griess reaction. Cytokine dosage was performed on frozen supernatants by
166 ELISA using DuoSet kits (R&D Systems), according to the manufacturer's instructions. NO and
167 cytokine concentrations were plotted both before and after normalization by cell viability.

168 **Viability and LDH release assays**. LDH release was measured using the CyQuant LDH Cytotoxicity
169 Assay kit (fresh supernatant) (Invitrogen), according to the manufacturers' instructions. Viability was
170 measured using MTT assay: cells were incubated for 2h in 1 mg/mL MTT solution (Sigma) in complete
171 RPMI. MTT crystals were then dissolved in HCl 1 M, isopropanol (1:24) and absorbance was read at
172 595 nm. For each technical replicate, the viability value was used to normalize both NO and cytokines
173 measurements using the following formula: $normalized\ value = \frac{NO/cytokine\ value}{MTT\ value}$.

174 **RT-qPCR.** RNAs were extracted from frozen cells using RNeasy Mini Kit (Qiagen) according to the
175 manufacturer's instructions. cDNAs were then obtained by retro-transcription (RT) using SuperScript II
176 RT (Invitrogen). The equivalent of 20ng of cDNA were used for RT-qPCR with specific primers and
177 probes (**Table 2**). qPCR was performed using Taqman Universal MasterMix (Applied Biosystems) on
178 a StepOne Plus Real Time PCR System (Applied Biosystems) with the standard protocol. Fold changes
179 were calculated with the $2^{-\Delta\Delta C_T}$ method, using hypoxanthine guanine phosphoribosyl transferase (HPRT)
180 as internal control.

181 **Statistical analyses.** All statistical analyses were performed using Student's *t*-test with
182 corresponding *p* values: * for $p < 0.05$; ** for $p < 0.01$ and *** for $p < 0.001$.

183

184 **RESULTS**

185 ***L. interrogans* induces upregulation and specific accumulation of autophagy-adaptor p62 in**
186 **puncta-like structures**

187 To address modulation of autophagy-adaptors upon infection with leptospires, we infected bone marrow
188 derived macrophages (BMDMs) with *L. interrogans* Manilae strain L495 and analyzed by Western blot
189 the levels of the different adaptors p62, NDP52 and Optineurin. We observed an accumulation of p62
190 over time upon infection (**Fig 1A**). We confirmed this phenotype using other pathogenic serotypes of
191 *L. interrogans*: Copenhageni strain Fiocruz L1-130 and Icterohaemorrhagiae strain Verdun, and using
192 the saprophytic *Leptospira biflexa* Patoc strain Patoc I (**Fig 1B**). Epifluorescence analyses of BMDMs
193 infected 4h with *L. interrogans* further revealed that infection triggers accumulation of p62 in puncta-
194 like structures (**Fig 1C**). This phenotype seemed specific of p62 since we did not observe accumulation
195 of the autophagy adaptors (NDP52 & optineurin) upon leptospira infection (**Sup. Fig 2A**).

196 Among other mechanisms, autophagy adaptors are constitutively degraded by autophagy upon
197 autophagosome / lysosome fusion. We hypothesized that p62 accumulation could be triggered by
198 blockage of autophagy flux by leptospires. However, when we monitored the autophagy hallmark
199 protein LC3-II in BMDMs by Western blot, no LC3-II accumulation was observed upon *Leptospira*
200 infection, in contrast to Bafilomycin (BafA1) treatment that blocks the autophagy flux, causing LC3-II
201 to accumulate (**Sup. Fig 1A**). Thus we conclude that infection with leptospires does not alter the
202 autophagy flux. Unexpectedly, we observed a mild reduction in LC3-II levels upon infection
203 (**Sup. Fig 1B**). Using murine macrophages RAW-mLC3-diFluo cells analyzed by automated
204 microscopy, we were able to confirm that leptospires induce a mild decrease of the number of
205 autophagosomes without altering the number of autolysosomes, again showing no alteration of the
206 autophagy flux (**Sup. Fig 1C-D**).

207 We then analyzed the transcriptional regulation of p62 in BMDMs by RT-qPCR and observed a
208 significant upregulation of p62 mRNA 24 h post-infection with *L. interrogans* (**Fig 1D**). This
209 corroborated the idea that p62 accumulation is not mediated by autophagy blockage. The kinetics of the
210 p62 puncta formation were further characterized in RAW264.7 cells, using automated high content (HC)

211 confocal microscopy. Results showed time-dependent increase of both the number of p62 puncta *per*
212 cell and the percentage of p62 positive cells (**Fig 1E & Sup. Fig 2B**). Single cell analysis confirmed an
213 average of 5-10 puncta *per* cell and highlighted cell-to-cell heterogeneity, with some macrophages
214 containing up to 60 puncta (**Fig 1F**). Of note, BafA1 that blocks autophagy flux also led to p62
215 accumulation as expected, but to a much lower extent than infection with leptospires (**Fig 1C, 1E & 1F**).
216 Altogether, these results confirm our previous results showing that *L. interrogans* do not induce
217 autophagy in murine macrophages (14), and suggest that leptospires induce a specific accumulation of
218 p62, not linked to an autophagy blockage.

219 **p62 accumulation is triggered by the leptospiral LPS through TLR4 & TLR2**

220 Many bacteria interfere actively with autophagy molecules *via* secreted effectors or RNA
221 interference (16, 23-28). To investigate whether such active mechanisms are also used by leptospires,
222 we analyzed BMDMs and RAW264.7 cells after stimulation with heat-killed (HK) leptospires. We
223 observed p62 accumulation visible by Western blot (**Fig 2A**) and quantified by automated microscopy
224 (**Fig 2B & 2C**). These findings exclude an active leptospiral mechanism and suggest a role for the
225 recognition of leptospiral MAMPs. We therefore stimulated cells for 24h with leptospiral LPS and
226 observed that such stimulation recapitulates p62 accumulation (**Fig 2A, 2B & 2C**). As p62 accumulation
227 seemed to be mediated by recognition of the leptospiral LPS, we investigated the roles of TLR4 &
228 TLR2. In murine cells, these two receptors are respectively activated by the leptospiral lipid A, and the
229 leptospiral lipoproteins that co-purify with the LPS (5, 12). We infected WT and TLR2/4 dko BMDMs
230 with *L. interrogans* for 24h, and analyzed by Western blot and automated microsopy. We observed that
231 p62 accumulation was greatly dampened in TLR2/TLR4 dko cells (**Fig 2D & 2E**). Finally, we analyzed
232 mRNA levels by RT-qPCR and observed that the increase in p62 mRNA levels observed in WT
233 BMDMs was abolished in TLR2/4 dko BMDMs (**Fig 2F**). Overall, these data show that p62
234 accumulation is mediated by TLR2/4 recognition of the leptospiral LPS. To address if such mechanism
235 was conserved *in vivo*, we injected C57BL/6 mice intraperitoneally with 1×10^8 heat-killed
236 *L. interrogans*, representative of MAMPs and potent TLR2/TLR4 agonists, that present the advantage

237 of not replicating nor disseminating upon injection. Interestingly, using automated microscopy we
238 showed that p62 was also accumulated *in vivo* in peritoneal F4/80^{+} macrophages (**Fig 2G**).

239 Finally, we ask whether this mechanism of p62 accumulation could be conserved in human
240 cells. Indeed, there is a TLR4 host species-specificity of the innate immune recognition of leptospires
241 (29). Leptospiral lipid A activates mouse-TLR4 but not human-TLR4 (12). However, lipoproteins that
242 co-purify with the LPS activate both mouse-TLR2 and human-TLR2 in a CD14-dependent manner (12).
243 We therefore infected human monocytic THP1-CD14 cells with *L. interrogans* serovar Manilae strain
244 L495. We also observed a specific p62 accumulation and no NDP52 accumulation after infection with
245 leptospires (**Sup. Fig 2C**), suggesting conserved mechanism of p62 accumulation in human and murine
246 macrophages, and a prominent role of TLR2 in human cells.

247 Leptospires have been shown to activate the NLRP3 inflammasome, in humans (30, 31), and in
248 a TLR2/4-dependent manner in mice (7). Furthermore, NLRP inflammasomes have been shown to
249 modulate autophagy (32-35). Therefore, we asked whether activation of inflammasome could play a
250 role in p62 accumulation and LC3-II diminution. We stimulated BMDMs with both live and heat-killed
251 leptospires in the presence or absence of NLRP3 inhibitor glibenclamide. Efficiency of the treatment
252 was controlled by measuring IL1β production after 24h (**Sup. Fig 3A**). p62 and LC3-II levels were
253 analyzed by Western blot. We observed a similar levels of p62 accumulation upon infection with either
254 live or heat-killed leptospires in both control and glibenclamide treated cells (**Sup. Fig 3B**).
255 Consistently, the diminution of LC3-II upon infection was visible in both control and glibenclamide
256 treated cells (**Sup. Fig 3B)**. Overall, this suggests that the modulation of autophagy players by
257 leptospires, although TLR2/4-dependent, is not mediated by activation of the NLRP3 inflammasome.

258 **Leptospires and their LPS trigger translocation of transcription factor NRF2**

259 Stress pathways are induced when autophagy adaptors accumulate in the cell (i.e. in the absence of
260 functional autophagy or because of specific upregulation). p62 accumulation induces translocation of
261 stress-responsive nuclear factor erythroid 2-related factor 2 (NRF2) (20, 36, 37). Subsequently, NRF2
262 triggers antioxidant and antiapoptotic programs (20, 36), and promotes p62 upregulation, creating a

263 loop that counteracts stress in autophagy-deficient conditions (36). We therefore infected BMDMs with
264 *L. interrogans* serovar Manilae strain L495 to analyze NRF2 by immunofluorescence 4h post-infection.
265 Whilst NRF2 staining was barely visible in the non-infected conditions, NRF2 staining in cell nuclei
266 was clearly evident upon infection (**Fig 3A**). The intensity of NRF2 staining in the nucleus peaked
267 around 4h post-infection (**Fig 3B**). We next performed single cell analysis of NRF2 fluorescence
268 intensity in the nucleus of RAW264.7 cells infected for 4h with three different serovars of
269 *L. interrogans*, and observed similar NRF2 increase for all the strains (**Fig 3C***, left panel*). Next, we
270 calculated the ratio of NRF2 intensities [nucleus/cytoplasm] and estimated that cells positive for NRF2
271 had a ratio > 1.4. We then plotted the percentage of cells with NRF2 ratio superior to 1.4 and observed
272 that up to 60% of cells were positive after 4h of infection (**Fig 3C***, right panel*). Finally, to understand
273 the contribution of leptospiral LPS in triggering NRF2, we performed similar analyses on BMDMs
274 stimulated for 4h with either live, heat-killed leptospires or their purified LPS. All conditions triggered
275 similar NRF2 translocation (**Fig 3D**), suggesting that the leptospiral LPS, that triggers accumulation of
276 p62, is responsible for NRF2 activation.

277 **p62 and NRF2 are in a feedback loop upon infection with leptospires**

278 Consequent to p62 accumulation and NRF2 translocation upon infection with *L. interrogans*, we
279 investigated the potential regulation mechanisms between these two phenotypes. We performed
280 small-interfering RNA (siRNA) transfection in BMDMs to knock-down specifically p62 or NRF2, and
281 analyzed NRF2 and p62 4h post-infection with leptospires by automated microscopy. We observed that
282 the NRF2 ratio [nucleus/cytoplasm] was lower upon infection in the p62 siRNA condition (**Fig 4A***, left*
283 *panel*). Conversely, p62 puncta formation was reduced upon infection in NRF2 siRNA transfected
284 BMDMs (**Fig 4B***, left panel*). Both p62 and NRF2 knocked-down were confirmed and quantified by
285 automated microscopy (**Fig 4A & 4B,** *right panels*). Overall, these results showed that p62 contributed
286 to NRF2 translocation, and that, in turn, NRF2 regulated p62 puncta formation, suggesting that p62 and
287 NRF2 are in a feedback loop upon infection by *L. interrogans*.

288 To further characterize the involvement of NRF2 in p62 activation, we analyzed BMDMs
289 transfected with NRF2 siRNA and infected with *L. interrogans* by Western blot and RT-qPCR 24h
290 post-infection, allowing us to measure both the protein and mRNA levels of p62. Interestingly, we
291 observed that NRF2 silencing prevented p62 protein accumulation (**Fig 4C**) but also reduced mRNA
292 upregulation (**Fig 4D**), suggesting that NRF2 is a transcriptional regulator of p62 activation.

293 **NRF2 translocation prevents inflammation upon infection**

294 NRF2 is a stress response transcription factor that promotes antioxidant and antiapoptotic programs
295 upon activation (20, 36). Therefore, we monitored the transcription of targets genes involved in fighting
296 oxidative stress in macrophages in response to infection. We infected BMDMs with *L. interrogans* and
297 analyzed the levels of glutathione S-reductase, catalase and heme oxygenase 1 mRNA by RT-qPCR at
298 4 h and 24 h post-infection. Interestingly, we observed no upregulation of these transcripts
299 (**Sup. Fig 4A, 4B & 4C**), suggesting that no antioxidant program is activated upon infection with
300 *L. interrogans*.

301 NRF2 has also been shown to have repressor functions and to dampen inflammation by
302 inhibiting the transcription of cytokines (38, 39), hence conferring resistance to inflammatory disease
303 such as sepsis (38). We therefore investigated the role of NRF2 translocation in inflammation upon
304 infection by leptospires. We transfected RAW264.7 cells with siRNA targeted against NRF2 and then
305 infected them with *L. interrogans*. As expected, considering that NRF2 is known to prevent cell death,
306 we observed a decrease in macrophage viability only upon infection of NRF2-silenced cells
307 (**Fig 5A***, left panel*). Interestingly, this enhanced loss of viability was not associated with lactate
308 dehydrogenase (LDH) release from the cytosol, illustrating that no membrane damage or cell lysis
309 occurred (**Fig 5A***, right panel*). We then analyzed the mRNA levels of several cytokines and enzymes,
310 namely iNOS (nitric oxide inducible synthase), IL6, TNF and IL10. Upon infection, all mRNA levels
311 were higher in NRF2-silenced cells than in control cells (**Fig 5B**), suggesting that NRF2 does play a role
312 in repressing the expression of inflammatory targets. Finally, to address whether this transcriptional
313 regulation was strong enough to alter cytokines levels, we analyzed nitric oxide (NO), IL6, TNF and

314 IL10 production in cell supernatant. Consistent with the mRNA analyses, we observed higher NO and
315 TNF upon infection of NRF2-silenced RAW264.7 (**Fig 5C**). These findings were even more striking
316 after normalizing cytokine production against cell viability, as measured using MTT
317 (**Fig 5C***, grey areas*). Increased levels of IL6 were observed after normalizing for cell viability, whereas
318 IL10 was not increased under any condition (**Fig 5C***, grey areas*). Overall, our results show that NRF2
319 plays a repressor role to dampen production of inflammatory mediators such as NO, TNF and IL6 in
320 mouse macrophages upon infection with *L. interrogans*.

321

322 **DISCUSSION**

323 Our results evidenced an accumulation of the autophagy adaptor p62 in puncta-like structures in
324 response to infection with both pathogenic *L. interrogans* and saprophytic *L. biflexa*. Classically,
325 autophagy adaptor p62 accumulates on the surface of intracellular bacteria, such as *Salmonella (16)*,
326 *Listeria* or *Shigella* (40) to target them to autophagosomes and it is associated with active modulation
327 of the autophagy flux through effectors (15, 16, 23, 27, 28). However, in the case of *Leptospira*, we
328 have previously published that leptospires actively enter but do not remain inside macrophages and are
329 not targeted by xenophagy (14). Moreover, the accumulation of p62 is also visible in response to
330 stimulation with extracellular heat-killed leptospires or with purified LPS through TLR2/TLR4, hence
331 excluding that only intracellular leptospires actively promote the formation of p62 puncta. This
332 hypothesis is consistent with the fact that leptospires do not possess traditional secretion systems (41)
333 used by other bacterial pathogens to modulate autophagy. Furthermore, our results showed that
334 leptospires do not alter autophagy flux in macrophages. These findings are in accordance with previous
335 studies from our laboratory showing that leptospires escape different innate immune
336 autophagy-activating pathways (15, 42), such as NOD-like receptors (8) and TLR4-TRIF (13). Overall,
337 we conclude that the leptospires behave differently from other pathogenic bacteria that actively
338 modulate autophagy, and for which p62 accumulates on the surface of intracellular bacteria.

339 We further demonstrated that p62 accumulation was induced by leptospiral LPS signaling
340 through TLR2/TLR4. The unique leptospiral LPS, the best characterized virulence factor (10), plays an
341 important role in leptospiral host-pathogen interactions. We previously showed that leptospiral LPS
342 avoids human TLR4 and mouse TLR4-TRIF activation (13). Recently, leptospiral LPS has also been
343 shown to prevent cell death by pyroptosis (43). Therefore, it was not surprising to find the leptospiral
344 LPS responsible for the p62-puncta phenotype. Interestingly, the LPS of *L. biflexa* has been shown to
345 be a more potent TLR4 agonist than the LPS of pathogenic *L. interrogans* (13), consistent with our
346 results showing greater p62 accumulation observed after infection with the saprophytic strain. Overall,
347 these findings are consistent with other studies reporting that p62 accumulates *via* TLR signaling (44),
348 directly through NFκB-mediated transcriptional regulation. We believe this could be the case upon
349 infection with leptospires because: *(i)* our results show an upregulation of p62 mRNA upon infection
350 and *(ii)* p62 levels upon infection are much higher than upon autophagy blockage with BafA1,
351 suggesting that the accumulation of p62 is not mediated by a dysregulation of autophagy.

352 TLR-induced accumulation of p62 has been shown to trigger the translocation of the
353 transcription factor NRF2 (44). Under physiological conditions, NRF2 is classically targeted for
354 degradation by the proteasome *via* interaction with its inhibitor Keap1 (37, 45). The accumulation and
355 direct binding of p62 to Keap1, leads to its sequestration and subsequent release from NRF2, which then
356 can translocate in the nucleus (20, 36, 37, 45). Our results confirmed that p62 induces translocation of
357 NRF2 upon infection with leptospires, and illustrated that the feedback loop between p62 and NRF2,
358 described in the literature (36), is activated upon *L. interrogans* infection. Interestingly, this loop has
359 few negative regulators, and it is hypothesized that its main regulator would be autophagy, through
360 degradation of p62 (36). Therefore, we hypothesize that since infection with leptospires does not trigger
361 autophagy, the feedback loop between p62 and NRF2 remains active, explaining why p62 puncta did
362 not disappear even at 24h post-infection. Overall, out data indicate that leptospires are potent activators
363 of the p62/NRF2 axis in macrophages.

364 Interestingly, NRF2 has also been shown to have transcription inhibition properties. In
365 BMDMs, NRF2 was described as an inhibitor of transcription for pro-inflammatory targets such as IL6,

366 IL1β and IL12 (39, 46). Our results showed that this is also the case upon infection with *L. interrogans*.
367 NRF2 inhibits polymerase III recruitment and hence prevents transcription of cytokines in response to
368 stimulation (39). Consequently, NRF2 was shown to downregulate neutrophils activation and
369 migration (47). Interestingly, although neutrophils are abundant in the blood of mice and humans
370 infected with leptospires, they are barely observed in the kidneys, the niche occupied by leptospires
371 during chronic infection (48, 49). Whether *Leptospira* modulate NRF2 translocation in neutrophils *via*
372 their LPS to favor survival in the kidneys remains to be studied. In addition, we showed that the
373 accumulation of p62 observed in murine macrophages was conserved in human cells. Interestingly,
374 human cells do not sense leptospiral lipid A through TLR4 (12), leading us to hypothesize that TLR2
375 alone could be responsible for sensing leptospires and inducing p62 accumulation in THP1 cells.
376 Although we could not address NRF2 translocation in human cells due to lack of specific tools, we
377 speculate that inflammation dampening might be conserved in human macrophages.

378 Other microbes such as Epstein-Barr virus (EBV) or parasite *Leshmania major* have been
379 shown to activate the p62/NRF2 axis (50, 51), hence showing an important role of NRF2 in response to
380 pathogens. However, to date, the role of NRF2 translocation in response to pathogens remains unclear.
381 Among others, NRF2 is involved in the induction of antioxidant program upon infection (36). We were
382 therefore surprised to observe no modulation in the mRNA levels of antioxidant targets upon infection.
383 Of note, pathogenic leptospires are equipped to fight against oxidative stress with inducible catalase, a
384 virulent factor, peroxidase, and peroxiredoxin (52). Interestingly, active repression of these
385 NRF2-dependent antioxidant targets was previously shown upon infection with live *Leshmania major*
386 parasite (51, 53). Whether leptospires could also actively prevent upregulation of NRF2 antioxidant
387 targets remains to be addressed.

388 In summary, we have demonstrated that leptospires passively subvert the p62-NRF2 axis
389 through LPS activation of TLR signaling and this leads to a reduction of inflammatory mediators. This
390 original mechanism might play a key role in the discretion of leptospires in hosts, evasion of immune
391 cell recruitment, and could potentially contribute to the establishment of chronic infections.

392

ACKNOWLEDGMENTS

We acknowledge Nathalie Aulner and Anne Danckaert (Institut Pasteur) as well as the Photonic BioImaging Unit of Technology and Service, a member of the France-BioImaging infrastructure, for support in conducting this study. We thank Richard Wheeler (Institut Pasteur) for critical reading of the manuscript and English editing.

STATEMENT OF ETHICS

All protocols were undertaken in compliance with EU Directive 2010/63 EU and the French regulation on the protection of laboratory animals issued on February 1st, 2013. They are part of project number # 2014-0049 and HA0036, which were approved by the Institut Pasteur ethics committee for animal experimentation (Comité d'Ethique en Expérimentation Animale CETEA registered under #89) and was authorized under #8562 by the French Ministry of Research, the French Competent Authority.

CONFLICT OF INTEREST STATEMENT

The authors have no conflicts of interest to declare.

FUNDING SOURCES

This work was funded by Institut Pasteur grant PTR2017-66 to CW and by Agence Nationale de la Recherche (ANR) grant ANR-10-LABX-62-IBEID to IGB. DB was funded by Université Paris Cité (formerly Université Paris Diderot) through Doctoral school FIRE (ED FIRE474). IS was part of the Pasteur-Paris University (PPU) International PhD program. This program received funding from the Institut Carnot Pasteur Microbes & Santé, and the European Union's Horizon 2020 research and innovation program under the Marie Sklodowska-Curie grant agreement no. 665807. IS additionally benefited from a scholarship "Fin de thèse de science" number FDT201805005258 granted by "Fondation pour la recherche médicale (FRM)". SP was supported by Université Paris Cité (formerly Université Paris Descartes) through doctoral school BioSPC (ED BIOSPC). The PE research was funded by the DARRI-Institut Carnot-*Microbe et santé* (grant number INNOV-SP10-19) and the ANR grant ANR-21-CE15-0038-01. France-BioImaging infrastructure network is supported by the French National Research Agency (ANR-10–INSB–04, Investments for the future). The use of the Opera Phenix system in the PBI core facility was made possible by the kind financial support of the Institut Pasteur (Paris) and the Région Ile-de-France (program DIM1Health).

AUTHORS CONTRIBUTIONS

Conception, administration, and supervision of the project: CW.

Investigation: DB, IS, SP and CW.

Methodology: IS, DB and PE.

Data analysis: DB, IS, PE and CW.

Visualization: DB.

Validation: IS, DB, SP and CW.

Resources: FVP.

Funding acquisition: CW and IGB.

DB and IS wrote the original draft, under CW's supervision.

All authors contributed to the review of the manuscript and approved it for submission.

DATA AVAILABILITY STATEMENT

All data generated or analysed during this study are included in this article. Further enquiries can be directed to the corresponding author.

REFERENCES

1. Costa F, Hagan JE, Calcagno J, Kane M, Torgerson P, Martinez-Silveira MS, et al. Global Morbidity and Mortality of Leptospirosis: A Systematic Review. PLoS Negl Trop Dis. 2015;9(9):e0003898.
2. Adler B. History of leptospirosis and *Leptospira*. Curr Top Microbiol Immunol. 2015;387:1-9.
3. Ko AI, Goarant C, Picardeau M. Leptospira: the dawn of the molecular genetics era for an emerging zoonotic pathogen. Nat Rev Microbiol. 2009;7(10):736-47.
4. Ratet G, Veyrier FJ, Fanton d'Andon M, Kammerscheit X, Nicola MA, Picardeau M, et al. Live imaging of bioluminescent *Leptospira interrogans* in mice reveals renal colonization as a stealth escape from the blood defenses and antibiotics. PLoS Negl Trop Dis. 2014;8(12):e3359.
5. Werts C, Tapping RI, Mathison JC, Chuang TH, Kravchenko V, Saint Girons I, et al. Leptospiral lipopolysaccharide activates cells through a TLR2-dependent mechanism. Nat Immunol. 2001;2(4):346-52.
6. Hsu SH, Hung CC, Chang MY, Ko YC, Yang HY, Hsu HH, et al. Active Components of *Leptospira* Outer Membrane Protein LipL32 to Toll-Like Receptor 2. Sci Rep. 2017;7(1):8363.
7. Lacroix-Lamande S, d'Andon MF, Michel E, Ratet G, Philpott DJ, Girardin SE, et al. Downregulation of the Na/K-ATPase pump by leptospiral glycolipoprotein activates the NLRP3 inflammasome. J Immunol. 2012;188(6):2805-14.
8. Ratet G, Santecchia I, Fanton d'Andon M, Vernel-Pauillac F, Wheeler R, Lenormand P, et al. LipL21 lipoprotein binding to peptidoglycan enables *Leptospira interrogans* to escape NOD1 and NOD2 recognition. PLoS Pathog. 2017;13(12):e1006725.

457 9. Holzapfel M, Bonhomme D, Cagliero J, Vernel-Pauillac F, Fanton d'Andon M, Bortolussi S, et al.
458 Escape of TLR5 Recognition by *Leptospira spp*.: A Rationale for Atypical Endoflagella. Front
459 Immunol. 2020;11:2007.

460 10. Murray GL, Srikram A, Henry R, Hartskeerl RA, Sermswan RW, Adler B. Mutations affecting
461 *Leptospira interrogans* lipopolysaccharide attenuate virulence. Mol Microbiol. 2010;78(3):701-9.

462 11. Que-Gewirth NL, Ribeiro AA, Kalb SR, Cotter RJ, Bulach DM, Adler B, et al. A methylated
463 phosphate group and four amide-linked acyl chains in *Leptospira interrogans* lipid A. The
464 membrane anchor of an unusual lipopolysaccharide that activates TLR2. J Biol Chem.
465 2004;279(24):25420-9.

466 12. Nahori MA, Fournie-Amazouz E, Que-Gewirth NS, Balloy V, Chignard M, Raetz CR, et al.
467 Differential TLR recognition of leptospiral lipid A and lipopolysaccharide in murine and human
468 cells. J Immunol. 2005;175(9):6022-31.

469 13. Bonhomme D, Santecchia I, Vernel-Pauillac F, Caroff M, Germon P, Murray G, et al. Leptospiral
470 LPS escapes mouse TLR4 internalization and TRIF-associated antimicrobial responses through O
471 antigen and associated lipoproteins. PLoS Pathog. 2020;16(8):e1008639.

472 14. Santecchia I, Bonhomme D, Papadopoulos S, Escoll P, Giraud-Gatineau A, Moya-Nilges M, et al.
473 Alive Pathogenic and Saprophytic Leptospires Enter and Exit Human and Mouse Macrophages
474 With No Intracellular Replication. Front Cell Infect Microbiol 2022;12:936931.

475 15. Travassos LH, Carneiro LA, Girardin S, Philpott DJ. Nod proteins link bacterial sensing and
476 autophagy. Autophagy. 2010;6(3):409-11.

477 16. Birmingham CL, Smith AC, Bakowski MA, Yoshimori T, Brumell JH. Autophagy controls
478 *Salmonella* infection in response to damage to the Salmonella-containing vacuole. J Biol Chem.
479 2006;281(16):11374-83.

480 17. Gutierrez MG, Master SS, Singh SB, Taylor GA, Colombo MI, Deretic V. Autophagy is a defense
481 mechanism inhibiting BCG and Mycobacterium tuberculosis survival in infected macrophages.
482 Cell. 2004;119(6):753-66.

483 18. Miyashita H, Oikawa D, Terawaki S, Kabata D, Shintani A, Tokunaga F. Crosstalk Between
484 NDP52 and LUBAC in Innate Immune Responses, Cell Death, and Xenophagy. Front Immunol.
485 2021;12:635475.

486 19. Moscat J, Diaz-Meco MT, Wooten MW. Of the atypical PKCs, Par-4 and p62: recent
487 understandings of the biology and pathology of a PB1-dominated complex. Cell Death Differ.
488 2009;16(11):1426-37.

489 20. Komatsu M, Kurokawa H, Waguri S, Taguchi K, Kobayashi A, Ichimura Y, et al. The selective
490 autophagy substrate p62 activates the stress responsive transcription factor NRF2 through
491 inactivation of Keap1. Nat Cell Biol. 2010;12(3):213-23.

492 21. Santecchia I, Vernel-Pauillac F, Rasid O, Quintin J, Gomes-Solecki M, Boneca IG, et al. Innate
493 immune memory through TLR2 and NOD2 contributes to the control of *Leptospira interrogans*
494 infection. PLoS Pathog. 2019;15(5):e1007811.

495 22. Bonhomme D, Werts C. Purification of LPS from *Leptospira*. Methods Mol Biol. 2020;2134:53-
496 65.

497 23. Birmingham CL, Canadien V, Gouin E, Troy EB, Yoshimori T, Cossart P, et al. *Listeria*
498 *monocytogenes* evades killing by autophagy during colonization of host cells. Autophagy.
499 2007;3(5):442-51.

24. Case ED, Chong A, Wehrly TD, Hansen B, Child R, Hwang S, et al. The *Francisella* O-antigen mediates survival in the macrophage cytosol via autophagy avoidance. Cell Microbiol. 2014;16(6):862-77.

25. Kreibich S, Emmenlauer M, Fredlund J, Ramo P, Munz C, Dehio C, et al. Autophagy Proteins Promote Repair of Endosomal Membranes Damaged by the Salmonella Type Three Secretion System 1. Cell Host Microbe. 2015;18(5):527-37.

26. Chen Z, Wang T, Liu Z, Zhang G, Wang J, Feng S, et al. Inhibition of Autophagy by MiR-30A Induced by *Mycobacteria tuberculosis* as a Possible Mechanism of Immune Escape in Human Macrophages. Jpn J Infect Dis. 2015;68(5):420-4.

27. Choy A, Dancourt J, Mugo B, O'Connor TJ, Isberg RR, Melia TJ, et al. The *Legionella* effector RavZ inhibits host autophagy through irreversible Atg8 deconjugation. Science. 2012;338(6110):1072-6.

28. Ogawa M, Yoshimori T, Suzuki T, Sagara H, Mizushima N, Sasakawa C. Escape of intracellular Shigella from autophagy. Science. 2005;307(5710):727-31.

29. Bonhomme D, Werts C. Host and Species-Specificities of Pattern Recognition Receptors Upon Infection With *Leptospira interrogans*. Front Cell Infect Microbiol. 2022;12:932137.

30. Li S, Wang M, Ojcius DM, Zhou B, Hu W, Liu Y, et al. Corrigendum to "*Leptospira interrogans* infection leads to IL-1beta and IL-18 secretion from a human macrophage cell line through reactive oxygen species and cathepsin B mediated-NLRP3 inflammasome activation" [Microbe Infect (2018) 254-260]. Microbes Infect. 2021;23(1):104756.

31. Li S, Wang M, Ojcius DM, Zhou B, Hu W, Liu Y, et al. *Leptospira interrogans* infection leads to IL-1beta and IL-18 secretion from a human macrophage cell line through reactive oxygen species and cathepsin B mediated-NLRP3 inflammasome activation. Microbes Infect. 2018;20(4):254-60.

32. Wlodarska M, Thaiss CA, Nowarski R, Henao-Mejia J, Zhang JP, Brown EM, et al. NLRP6 inflammasome orchestrates the colonic host-microbial interface by regulating goblet cell mucus secretion. Cell. 2014;156(5):1045-59.

33. Jounai N, Kobiyama K, Shiina M, Ogata K, Ishii KJ, Takeshita F. NLRP4 negatively regulates autophagic processes through an association with beclin1. J Immunol. 2011;186(3):1646-55.

34. Deng Q, Wang Y, Zhang Y, Li M, Li D, Huang X, et al. *Pseudomonas aeruginosa* Triggers Macrophage Autophagy To Escape Intracellular Killing by Activation of the NLRP3 Inflammasome. Infect Immun. 2016;84(1):56-66.

35. Lai M, Yao H, Shah SZA, Wu W, Wang D, Zhao Y, et al. The NLRP3-Caspase 1 Inflammasome Negatively Regulates Autophagy via TLR4-TRIF in Prion Peptide-Infected Microglia. Front Aging Neurosci. 2018;10:116.

36. Jain A, Lamark T, Sjottem E, Larsen KB, Awuh JA, Overvatn A, et al. p62/SQSTM1 is a target gene for transcription factor NRF2 and creates a positive feedback loop by inducing antioxidant response element-driven gene transcription. J Biol Chem. 2010;285(29):22576-91.

37. Lau A, Wang XJ, Zhao F, Villeneuve NF, Wu T, Jiang T, et al. A noncanonical mechanism of Nrf2 activation by autophagy deficiency: direct interaction between Keap1 and p62. Mol Cell Biol. 2010;30(13):3275-85.

38. Kong X, Thimmulappa R, Craciun F, Harvey C, Singh A, Kombairaju P, et al. Enhancing Nrf2 pathway by disruption of Keap1 in myeloid leukocytes protects against sepsis. Am J Respir Crit Care Med. 2011;184(8):928-38.

543 39. Kobayashi EH, Suzuki T, Funayama R, Nagashima T, Hayashi M, Sekine H, et al. Nrf2 suppresses
544 macrophage inflammatory response by blocking proinflammatory cytokine transcription. Nat
545 Commun. 2016;7:11624.

546 40. Mostowy S, Sancho-Shimizu V, Hamon MA, Simeone R, Brosch R, Johansen T, et al. p62 and
547 NDP52 proteins target intracytosolic *Shigella and Listeria* to different autophagy pathways. J Biol
548 Chem. 2011;286(30):26987-95.

549 41. Abby SS, Cury J, Guglielmini J, Neron B, Touchon M, Rocha EP. Identification of protein secretion
550 systems in bacterial genomes. Sci Rep. 2016;6:23080.

551 42. Xu Y, Jagannath C, Liu XD, Sharafkhaneh A, Kolodziejska KE, Eissa NT. Toll-like receptor 4 is
552 a sensor for autophagy associated with innate immunity. Immunity. 2007;27(1):135-44.

553 43. Bonhomme D, Hernandez-Trejo V, Papadopoulos S, Pigache R, Fanton d'Andon M, Outlia A, et
554 al. *Leptospira interrogans* prevents macrophage cell death and pyroptotic IL1ß release through
555 atypical lipopolysaccharide. J Immunol. 2023;210:1-16.

556 44. Yin S, Cao W. Toll-Like Receptor Signaling Induces Nrf2 Pathway Activation through p62-
557 Triggered Keap1 Degradation. Mol Cell Biol. 2015;35(15):2673-83.

558 45. Jiang T, Harder B, Rojo de la Vega M, Wong PK, Chapman E, Zhang DD. p62 links autophagy
559 and Nrf2 signaling. Free Radic Biol Med. 2015;88(Pt B):199-204.

560 46. Macoch M, Morzadec C, Genard R, Pallardy M, Kerdine-Romer S, Fardel O, et al. Nrf2-dependent
561 repression of interleukin-12 expression in human dendritic cells exposed to inorganic arsenic. Free
562 Radic Biol Med. 2015;88(Pt B):381-90.

563 47. Helou DG, Braham S, De Chaisemartin L, Granger V, Damien MH, Pallardy M, et al. Nrf2
564 downregulates zymosan-induced neutrophil activation and modulates migration. PLoS One.
565 2019;14(8):e0216465.

566 48. Fanton d'Andon M, Quellard N, Fernandez B, Ratet G, Lacroix-Lamande S, Vandewalle A, et al.
567 *Leptospira Interrogans* induces fibrosis in the mouse kidney through Inos-dependent, TLR- and
568 NLR-independent signaling pathways. PLoS Negl Trop Dis. 2014;8(1):e2664.

569 49. Raffray L, Giry C, Vandroux D, Kuli B, Randrianjohany A, Pequin AM, et al. Major Neutrophilia
570 Observed in Acute Phase of Human Leptospirosis Is Not Associated with Increased Expression of
571 Granulocyte Cell Activation Markers. PLoS One. 2016;11(11):e0165716.

572 50. Gilardini Montani MS, Santarelli R, Granato M, Gonnella R, Torrisi MR, Faggioni A, et al. EBV
573 reduces autophagy, intracellular ROS and mitochondria to impair monocyte survival and
574 differentiation. Autophagy. 2019;15(4):652-67.

575 51. Bichiou H, Rabhi S, Ben Hamda C, Bouabid C, Belghith M, Piquemal D, et al. *Leishmania*
576 Parasites Differently Regulate Antioxidant Genes in Macrophages Derived From Resistant and
577 Susceptible Mice. Front Cell Infect Microbiol. 2021;11:748738.

578 52. Zavala-Alvarado C, Sismeiro O, Legendre R, Varet H, Bussotti G, Bayram J, et al. The
579 transcriptional response of pathogenic *Leptospira* to peroxide reveals new defenses against
580 infection-related oxidative stress. PLoS Pathog. 2020;16(10):e1008904.

581 53. Vivarini AC, Calegari-Silva TC, Saliba AM, Boaventura VS, Franca-Costa J, Khouri R, et al.
582 Systems Approach Reveals Nuclear Factor Erythroid 2-Related Factor 2/Protein Kinase R
583 Crosstalk in Human Cutaneous Leishmaniasis. Front Immunol. 2017;8:1127.

584

585

586 **FIGURES & LEGENDS**

587 **Figure 1.**

588

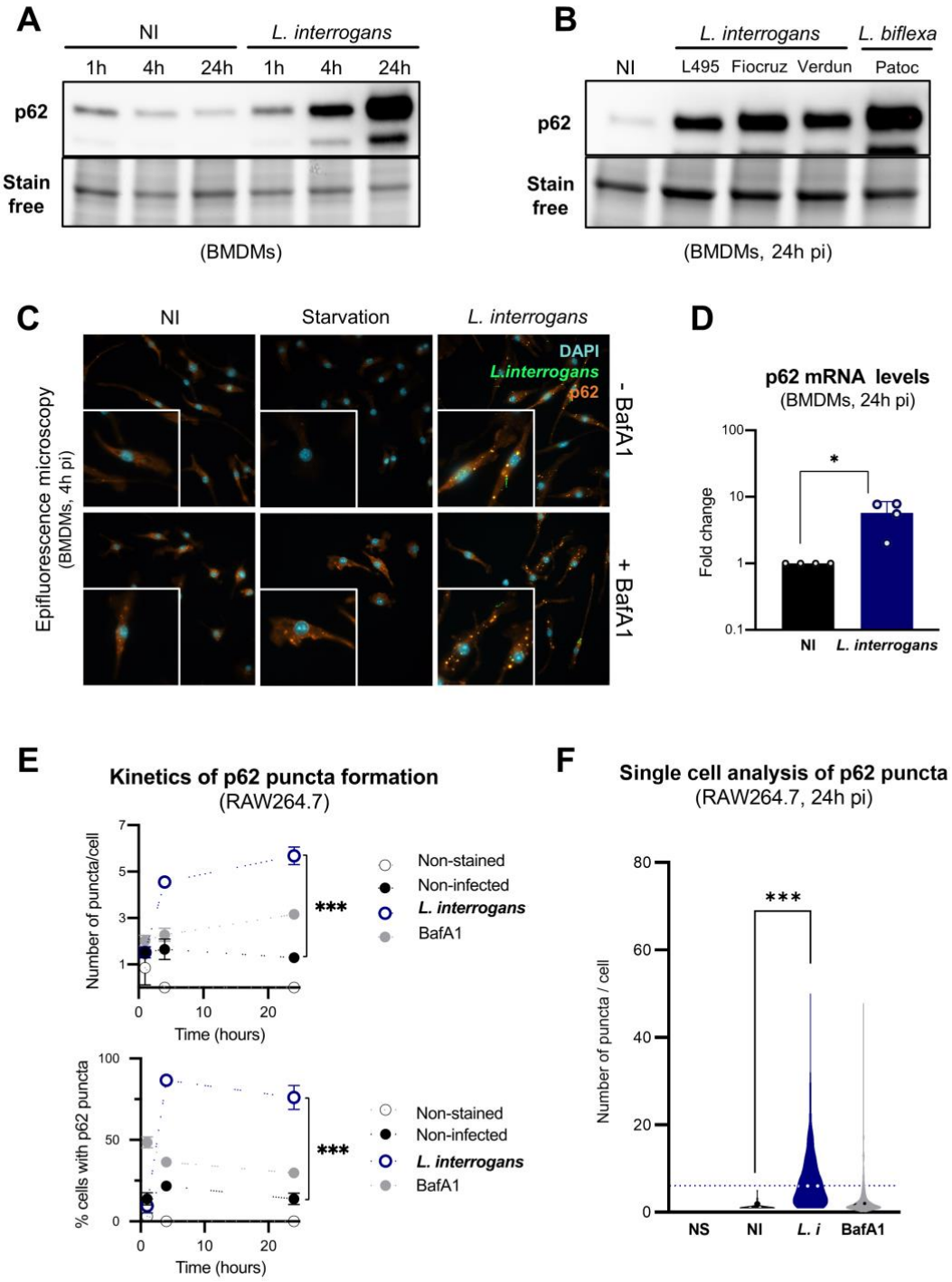

Figure 1. *L. interrogans* induces upregulation and specific accumulation of autophagy-adaptor p62 in puncta-like structures

A) WB of p62 in BMDMs 1h, 4h and 24h post-infection with *L. interrogans* serovar Manilae strain L495 at MOI 100. Gel stain free is presented as loading control of total proteins. **B)** WB of p62 in BMDMs 24h post-infection with *L. interrogans* serovar Manilae strain L495, serovar Copenhageni strain Fiocruz L1-130, serovar Icterohaemorrhagiae strain Verdun, and *L. biflexa* serovar Patoc strain Patoc I, at MOI 100. **C)** Epifluorescence analyses of p62 in BMDMs 4h post-infection with fluorescently-labeled *L. interrogans* serovar Manilae strain L495 at MOI 10, or 4h upon starvation induction in EBSS medium, with or without 100nM of bafilomycin A1 (BafA1). **D)** RT-qPCR analyses of p62 mRNA levels in BMDMs 24h post-infection with *L. interrogans* serovar Manilae strain L495 at MOI 100. Bars correspond to mean +/- SD of technical replicates (n=4). **E)** Automated confocal microscopy analyses of the number of p62 puncta *per* cell and the percentage of p62 positive cells in RAW264.7 cells 1h, 4h and 24h post-infection with *L. interrogans* serovar Manilae strain L495 at MOI 100, or stimulation with 100nM of BafA1. Dots correspond to mean +/- SD of technical replicates (n=3). **F)** Single cell microscopy analysis of the number of p62 puncta *per* cell 24h post-infection of RAW264.7 cells with *L. interrogans* serovar Manilae strain L495 at MOI 100, or stimulation with 100nM of BafA1. Dashed lines correspond to median. **A-F)** Data presented are representative of at least 3 independent experiments. Statistical analyses were performed using Student's *t*-test with corresponding p values:* for $p < 0.05$ and *** for $p < 0.001$.

609 **Figure 2.**

610

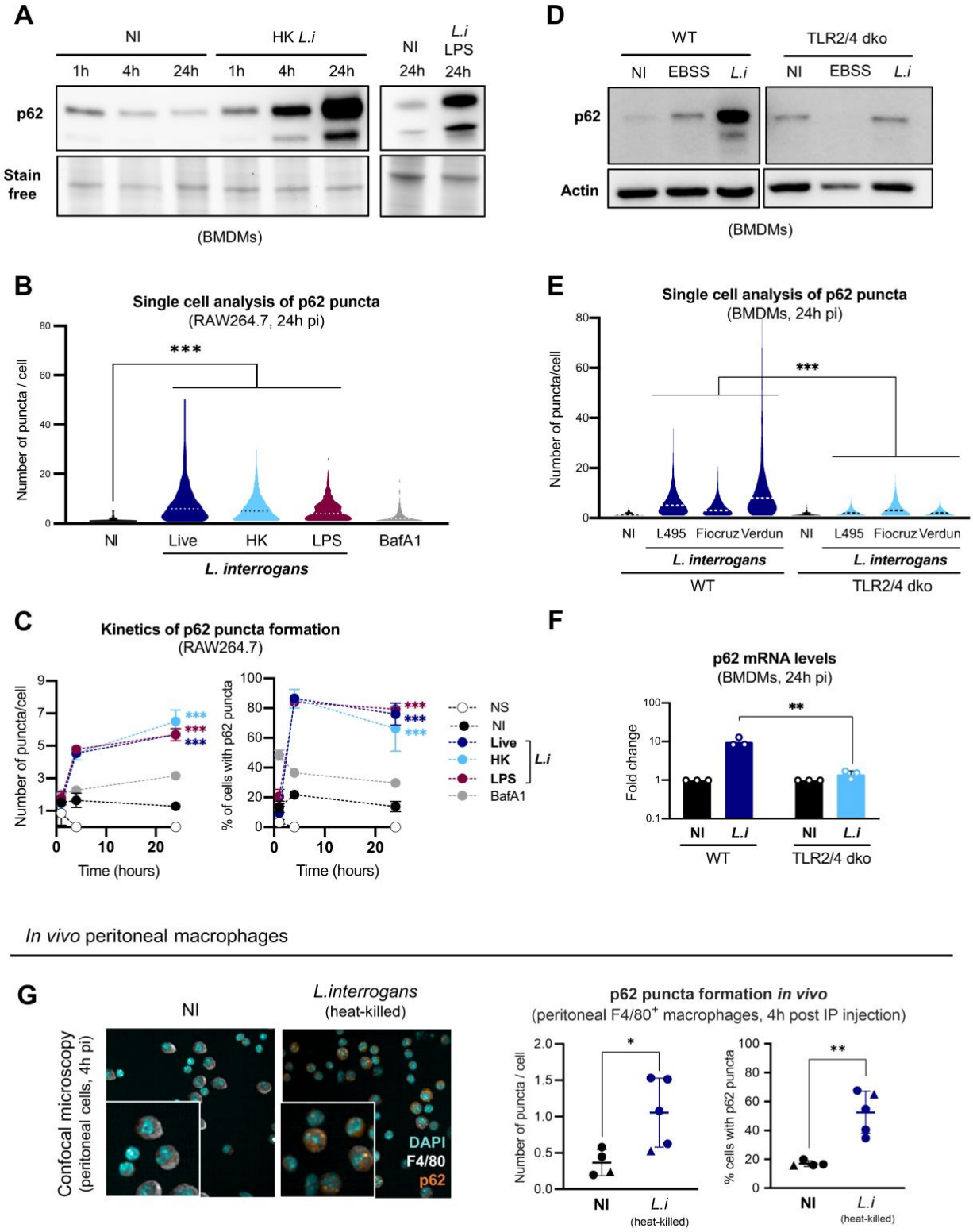

Figure 2. p62 accumulation is triggered by the leptospiral LPS through TLR4 & TLR2

A) WB of p62 in BMDMs 1h, 4h and 24h post-stimulation with heat-killed (56°C, 30 min) *L. interrogans* serovar Manilae strain L495 at MOI 100 or 24 h post-stimulation with 1 µg/mL of the corresponding purified leptospiral LPS. Gel stain free is presented as a loading control of total proteins. **B)** Single cell microscopy analysis of the number of p62 puncta *per* cell 24h post-infection of RAW264.7 cells with either live or heat-killed (56°C, 30 min) *L. interrogans* serovar Manilae strain L495 at MOI 100, stimulation with 1 µg/mL of the corresponding purified leptospiral LPS, or stimulation with 100nM of bafilomycin A1 (BafA1). Dashed lines correspond to median. **C)** Automated confocal microscopy analyses of the number of p62 puncta *per* cell and the percentage of p62 positive cells 1h, 4h and 24h post-stimulation of RAW264.7 cells with MOI 100 of either live or heat-killed (56°C, 30 min) *L. interrogans* serovar Manilae strain L495, stimulation with 1 µg/mL of the corresponding purified leptospiral LPS, or stimulation with 100nM of BafA1. Dots correspond to mean +/- SD of technical replicates (n=3). **D)** WB of p62 in WT and TLR2/4 dko BMDMs 24h post-infection with *L. interrogans* serovar Manilae strain L495 at MOI 100, or upon starvation induction in EBSS medium. WB of actin is presented as loading control. **E)** Single cell microscopy analysis of the number of p62 puncta *per* cell 24h post-infection of WT and TLR2/4 dko BMDMs with *L. interrogans* serovar Manilae strain L495, serovar Copenhageni strain Fiocruz L1-130 or serovar Icterohaemorrhagiae strain Verdun at MOI 100. Dashed lines correspond to median. **F)** RT-qPCR analyses of p62 mRNA levels in WT and TLR2/4 dko BMDMs 24h post-infection with *L. interrogans* serovar Manilae strain L495 at MOI 100. Bars correspond to mean of independent experiments (n=3). **G)** Automated confocal microscopy images and analyses of the number of p62 puncta *per* cell and the percentage of p62 positive cells in adherent F4/80^{+} peritoneal cells 4h post intra-peritoneal injection of 1 x10^{8} heat-killed (56°C, 30 min) *L. interrogans* serovar Manilae strain L495 in C57BL/6J mice. Dots correspond to individual mice from 3 independent experiments (round symbols = females / triangle symbols = males). **A-C, F, G)** Data presented are representative of at least 3 independent experiments. **D-E)** Data presented are representative of 2 independent experiments. Statistical analyses were performed using Student's *t*-test with corresponding p values: * for $p < 0.05$; ** for $p < 0.01$ and *** for $p < 0.001$.

638 **Figure 3.**

639

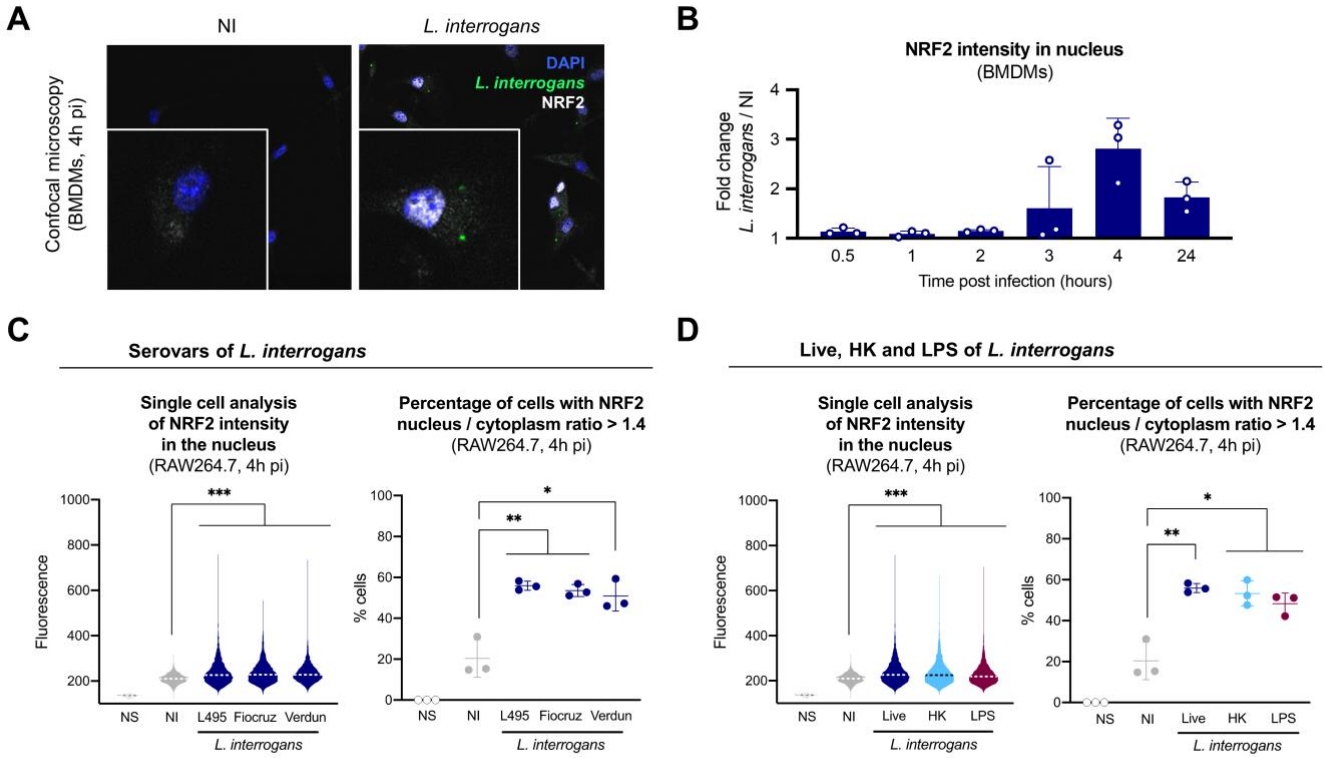

Figure 3. Leptospires and their LPS trigger translocation of transcription factor NRF2

A) Confocal microscopy analyses of NRF2 in BMDMs 4h post-infection with *L. interrogans* serovar Manilae strain L495 at MOI 100. **B)** Automated confocal microscopy analyses of NRF2 intensity 0.5h, 1h, 2h, 4h and 24h post-infection of BMDMs with *L. interrogans* serovar Manilae strain L495 at MOI 100. Fluorescence values of infected cells were normalized by non-infected cells. Bars correspond to mean +/- SD of technical replicates (*n*=3). **C) Left panel.** Single cell microscopy analysis of NRF2 intensity in the nucleus 4h post-infection of RAW264.7 cells with *L. interrogans* serovar Manilae strain L495, serovar Copenhageni strain Fiocruz L1-130 or serovar Icterohaemorrhagiae strain Verdun at MOI 100. Fluorescence is expressed in arbitrary units (AU). Dashed lines correspond to median. **Right panel.** Automated confocal microscopy analysis of the number of cells with NRF2 intensity ratio [nucleus/cytoplasm] > 1.4 4h post-infection of RAW264.7 cells with *L. interrogans* serovar Manilae strain L495, serovar Copenhageni strain Fiocruz L1-130 or serovar Icterohaemorrhagiae strain Verdun at MOI 100. Lines correspond to mean +/- SD of technical replicates (*n*=3). **D) Left panel.** Single cell microscopy analysis of NRF2 intensity in the nucleus 4h post-infection of RAW264.7 cells with MOI 100 of either live or heat-killed (56°C, 30 min) *L. interrogans* serovar Manilae strain L495 or stimulation with 1 µg/mL of the corresponding purified leptospiral LPS. Fluorescence is expressed in arbitrary units (AU). Dashed lines correspond to median. **Right panel.** Automated confocal microscopy analysis of the number of cells with NRF2 intensity ratio [nucleus/cytoplasm] > 1.4 4h post-infection of RAW264.7 cells with MOI 100 of either live or heat-killed (56°C, 30 min) *L. interrogans* serovar Manilae strain L495 or stimulation with 1 µg/mL of the corresponding purified leptospiral LPS. Lines correspond to mean +/- SD of technical replicates (*n*=3). **A-D)** Data presented are representative of at least 2 independent experiments.

663 **Figure 4.**

664

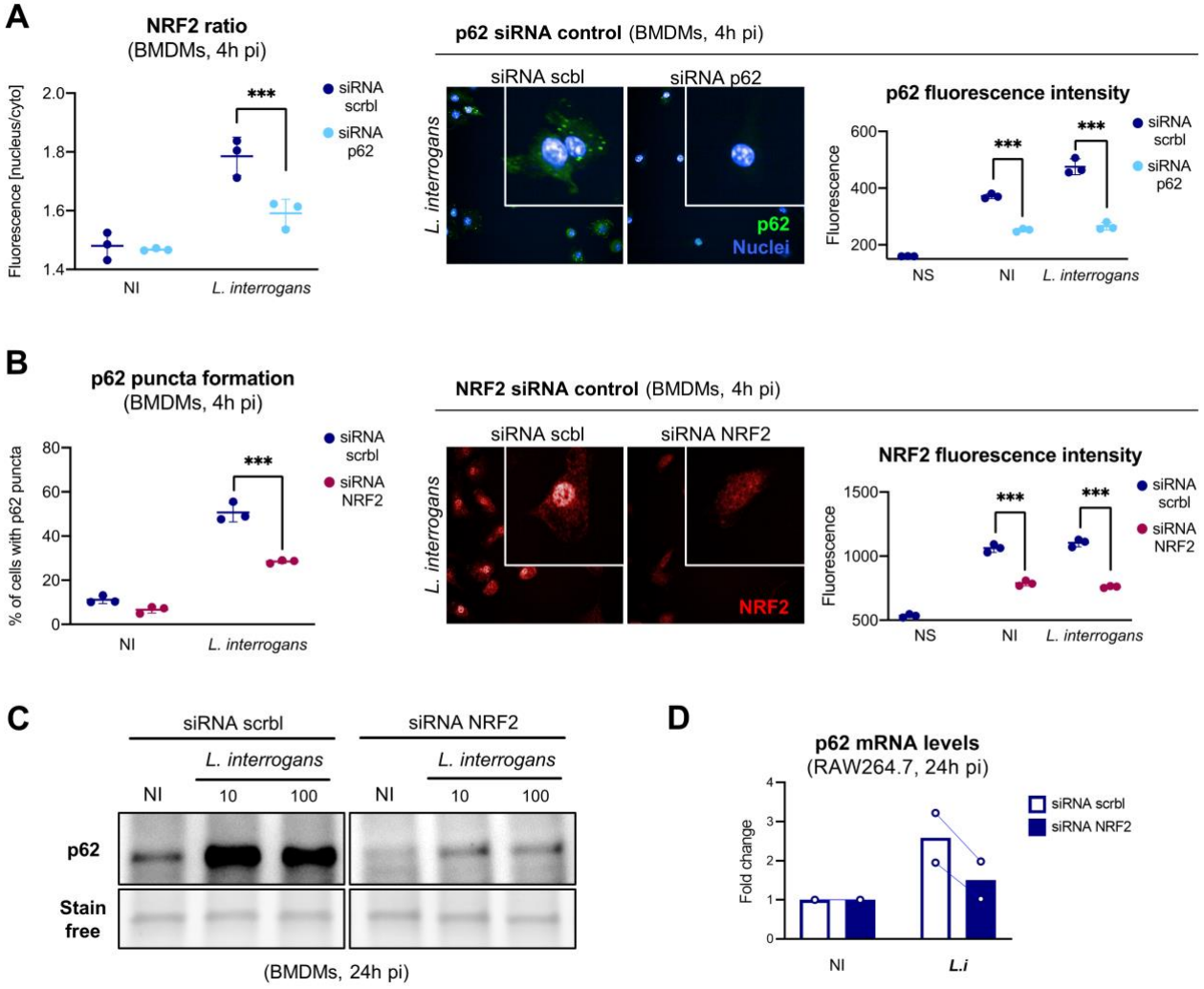

Figure 4. p62 and NRF2 are in a feedback loop upon infection with leptospires

A) Left panel. Automated confocal microscopy analysis of NRF2 intensity ratio [nucleus/cytoplasm] in BMDMs transfected with scramble (scrbl) or p62 siRNA and infected for 4h with *L. interrogans* serovar Manilae strain L495 at MOI 100. Lines correspond to mean +/- SD of technical replicates (*n*=3). **Right panel.** Corresponding controls are microscopy analyses and quantification of p62 intensity in the same transfection and infection conditions. Lines correspond to mean +/- SD of technical replicates (*n*=3). **B) Left panel.** Automated confocal microscopy analysis of p62 puncta formation in BMDMs transfected with scrbl or NRF2 siRNA and infected for 4h with *L. interrogans* serovar Manilae strain L495 at MOI 100. Lines correspond to mean +/- SD of technical replicates (*n*=3). **Right panel.** Corresponding controls are microscopy analyses and quantification of NRF2 intensity in the same transfection and infection conditions. Lines correspond to mean +/- SD of technical replicates (*n*=3). **C)** WB of p62 in BMDMs transfected with scrbl or NRF2 siRNA and infected for 24h with *L. interrogans* serovar Manilae strain L495 at MOI 10 or 100. **D)** RT-qPCR analyses of p62 mRNA levels in RAW264.7 cells transfected with scrbl or NRF2 siRNA and infected for 24h with *L. interrogans* serovar Manilae strain L495 at MOI 100. Bars correspond to mean of independent experiments (*n*=2). **A-B)** Data presented are representative of at least 3 independent experiments. **C-D)** Data presented are representative of 2 independent experiments. Statistical analyses were performed using Student's *t*-test with corresponding *p* values: *** for $p < 0.001$.

684 **Figure 5.**

685

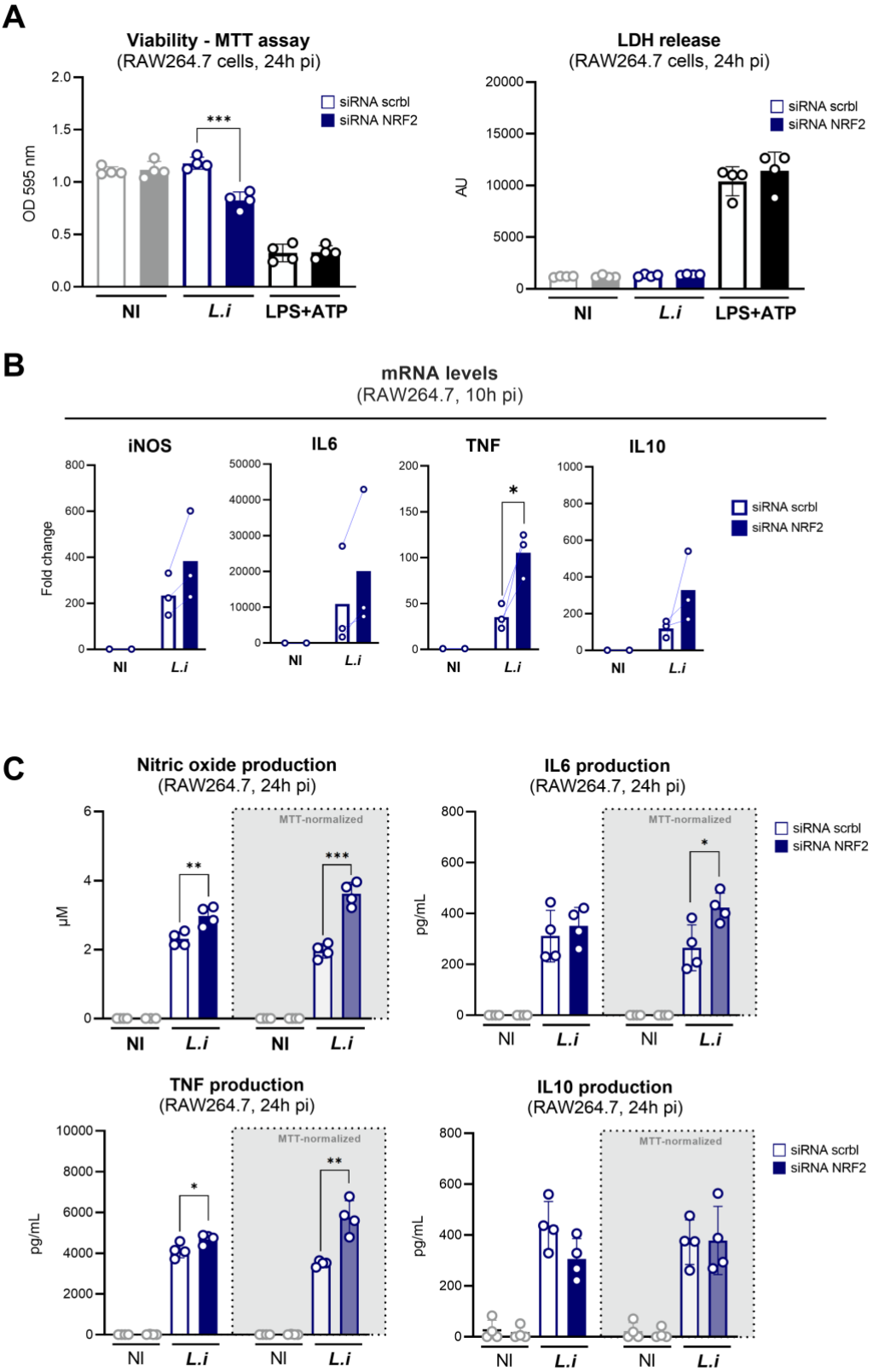

Figure 5. NRF2 translocation prevents inflammation upon infection

A) Cell viability (measured by MTT assay) and LDH release (measured by CyQuant assay) in RAW264.7 cells transfected with scramble (scrbl) or NRF2 siRNA and infected for 24h with *L. interrogans* serovar Manilae strain L495 at MOI 100 or stimulated with positive control for lytic cell death: LPS of *E. coli* 1µg/mL + ATP 5mM. Bars correspond to mean +/- SD of technical replicates (n=4). **B)** RT-qPCR analyses of iNOS, IL6, TNF and IL10 mRNA levels in RAW264.7 cells transfected with scrbl or NRF2 siRNA and infected for 10h with *L. interrogans* serovar Manilae strain L495 at MOI 100. Bars correspond to mean of independent experiments (n=3). **C)** NO dosage by Griess reaction and, IL6, TNF and IL10 dosages by ELISA in RAW264.7 cells transfected with scrbl or NRF2 siRNA and infected for 24h with *L. interrogans* serovar Manilae strain L495 at MOI 100. Bars correspond to mean +/- SD of technical replicates (n=4). **A-C)** Data presented are representative of at least 3 independent experiments. Statistical analyses were performed using Student's *t*-test with corresponding p values: * for $p < 0.05$; ** for $p < 0.01$ and *** for $p < 0.001$.

700 **TABLES**

701

702 **Table 1.** Antibodies list for immunofluorescence and Western blot analyses

Application*	Target	Clonality**	Conjugated	Host	Dilution	Reference	Supplier
IF	**p62**	mAb	No	Rabbit	1:500	ab109012	Abcam
	Rabbit IgG	pAb	AlexaFluor 488	Goat	1:1.000	A-11034	ThermoFisher
IF	**Nrf2**	mAb	No	Rat	1:250	#14596	CST
	Rat IgG	pAb	AlexaFluor 647	Goat	1:1.000	A-21247	ThermoFisher
IF	**F4/80**	mAb	APC-Cyanine7	Rat	1:250	123117	BioLegend
WB	**LC3**	pAb	Purified	Rabbit	1:1.000	L7543	Sigma
	p62	mAb	Purified	Mouse	1:1.000	ab109012	Abcam
	OPTN	pAb	Purified	Rabbit	1:1.000	ab23666	Abcam
	NDP52	pAb	Purified	Rabbit	1:1.000	GTX115378	GeneTex
	Rabbit IgG	pAb	HRP	Goat	1:10.000	7074S	CST

703 * IF: immunofluorescence, WB: Western blot, ** mAb: monoclonal antibody, pAb: polyclonal antibody

704

705 **Table 2.** Primers and probe list for RT-qPCR analyses

Target	Forward primer sequence	Reverse primer sequence	Probe sequence
p62	5'-ATGTGGAACATGGAGGGAAGAG-3'	5'-TTCTGTGCCTGTGCTGGAACT-3'	5'-CCGCCTGACACCCACTACCCCA-3'
lc3	5'-GCCCCACCCCTGAAAGG-3'	5'-TGCAGAGGAAATGACCACAGAT-3'	5'-TGGCTCCCCTTGTCCTGACTCGG-3'
iNOS	5'-CATGACTGCTAATGTCAGAG-3'	5'-TCCTAGTCCATCCGGATAAA-3'	5'-GAAATCTGAGTTTGGCCTGAGG-3'
tnf	5'-CATCTTCTCAAAATTCGAGTGACAA-3'	5'-TGGGAGTAGACAAGGTACAACCC-3'	5'-CACGTCGTAGCAAACCACCAAGTGGA-3'
il6	5'-CTCCAGCTTATCTGTTAGGA-3'	5'-CTTCAACCAAGAGGTAAAAGA-3'	5'-AAATTGGGGTAGGAAGGACTATTTTATG-3'
il10	5'-GGCGCTGTCATCGATTTCTC-3'	5'-GACACCTTGGTCTTGGAGCTTATTAA-3'	5'-AAAATAAGAGCAAGGCAGTGGAGCAGGTG-3'
hprt	5'-CTGGTGAAAAGGACCTCTCGA-3'	5'-TGCCCTTGACTATAATGAGTACTTCA-3'	5'-TGTTGGATACAGGCCAGACTTTGTTGGAT-3'
cat	Pre-designed: Mm00437992_m1 (ThermoFisher)		
gsr	Pre-designed: Mm01197925_m1 (ThermoFisher)		
hprt	Pre-designed: Mm03024075_m1 (ThermoFisher)		

706

Sup. Figures 1-4

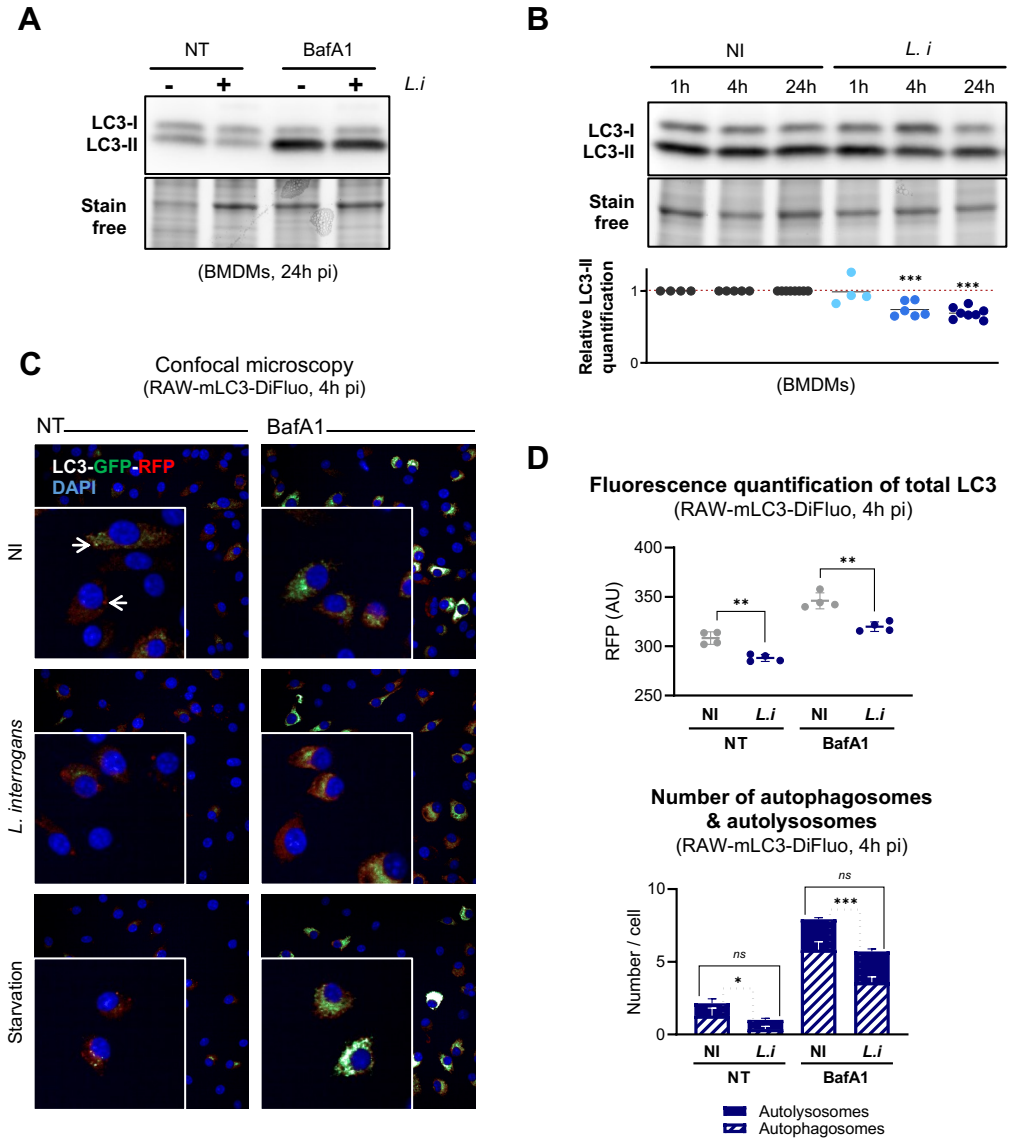

Sup. Figure 1. *L. interrogans* does not induce autophagy in murine macrophages and reduces the number of autophagosomes

A) WB of LC3 in BMDMs 24h post-infection with *L. interrogans* serovar Manilae strain L495 at MOI 100 with or without addition of bafilomycin A1 (BafA1) 4h prior to cell collection. **B)** WB and quantification of LC3 in BMDMs 1h, 4h or 24h post-infection with *L. interrogans* serovar Manilae strain L495 at MOI 100. Quantifications represent the ratio of LC3-II in stimulated cells over non-stimulated cells, and after gel stain free normalization. Each dot corresponds to the quantification of a WB from an independent experiment. **C-D)** Automated confocal microscopy images and quantifications of RAW-mLC3-DiFluo cells 4h post-infection with *L. interrogans* serovar Manilae strain L495 at MOI 100, or post starvation induction in EBSS medium, with or without BafA1 addition 2h before cell fixation. Of note, RAW-mLC3-DiFluo cells are stably transfected with LC3 tagged with tandem GFP-RFP. Both GFP and RFP are fluorescent under basal conditions, however, GFP fluorescence is quenched during acidification of autophagosomes upon fusion with lysosomes. Total LC3 fluorescence was measured based on RFP signal. Autophagosomes were quantified as RFP^+/GFP^+ punctas (upper white arrow) whereas autolysosomes were quantified as GFP^-/RFP^+ punctas (lower white arrow). Lines and bars correspond to mean +/- SD of technical replicates (n=4). **A-D)** Statistical analyses were performed using Student's t-test with corresponding p values: * for $p < 0.05$; ** for $p < 0.01$ and *** for $p < 0.001$.

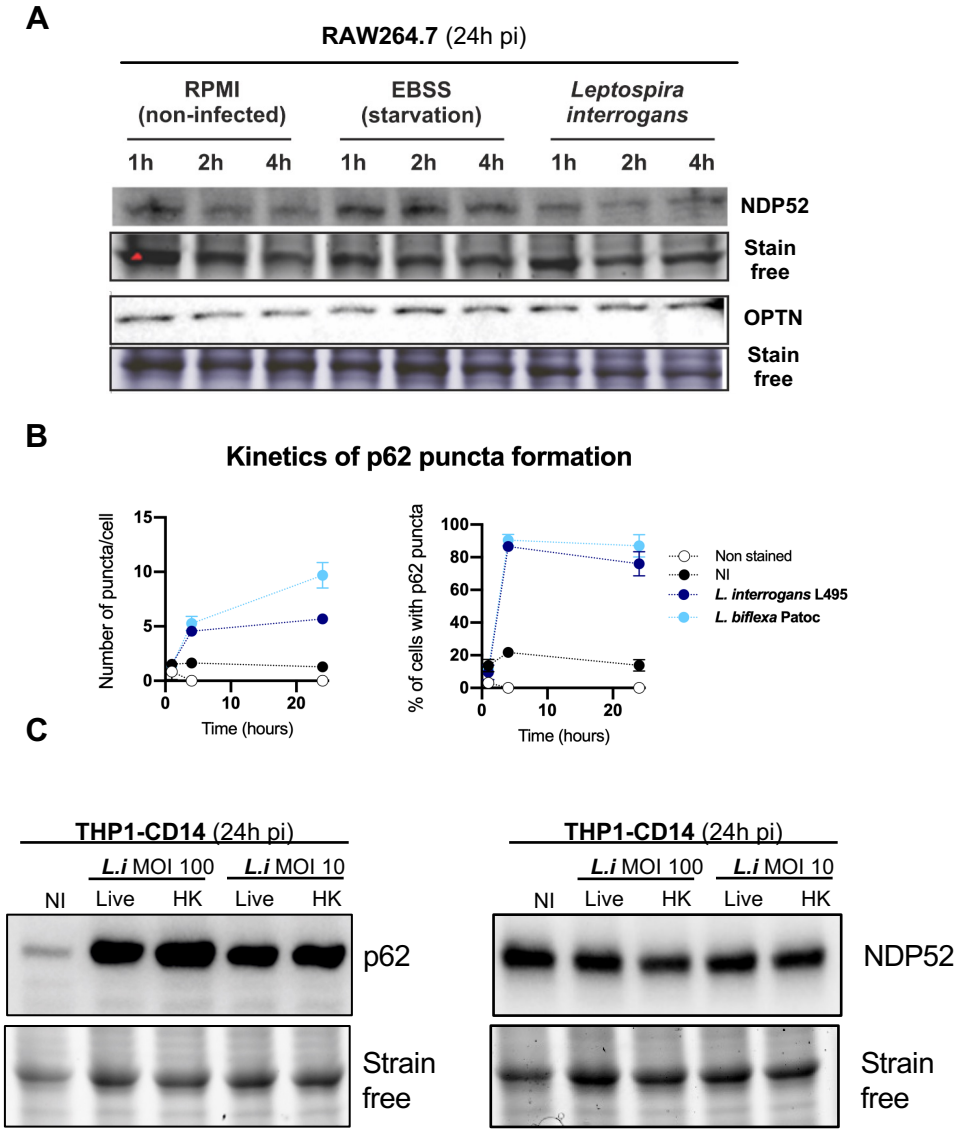

Sup. Figure 2. Specific p62 accumulation is observed in murine and human cells

A) WB of NDP52 and OPTN in RAW264.7 cells 1h, 2h and 4h post-infection with *L. interrogans* serovar Manilae strain L495 at MOI 100, or upon starvation induction in EBSS medium. **B)** Automated microscopy analyses of the number of p62 puncta *per* cell and the percentage of p62 positive cells 1h, 4h and 24h post-infection of RAW264.7 cells with *L. interrogans* serovar Manilae strain L495 or *L. biflexa* serovar Patoc strain Patoc I, at MOI 100. Dots correspond to mean +/- SD of technical replicates (n=3). Statistical analyses were performed using Student's t-test with corresponding p values: * for $p < 0.05$; ** for $p < 0.01$ and *** for $p < 0.001$. **C)** WB of p62 and NDP52 in human THP1-CD14 cells 24h post-infection with *L. interrogans* serovar Manilae strain L495 at MOI 100.

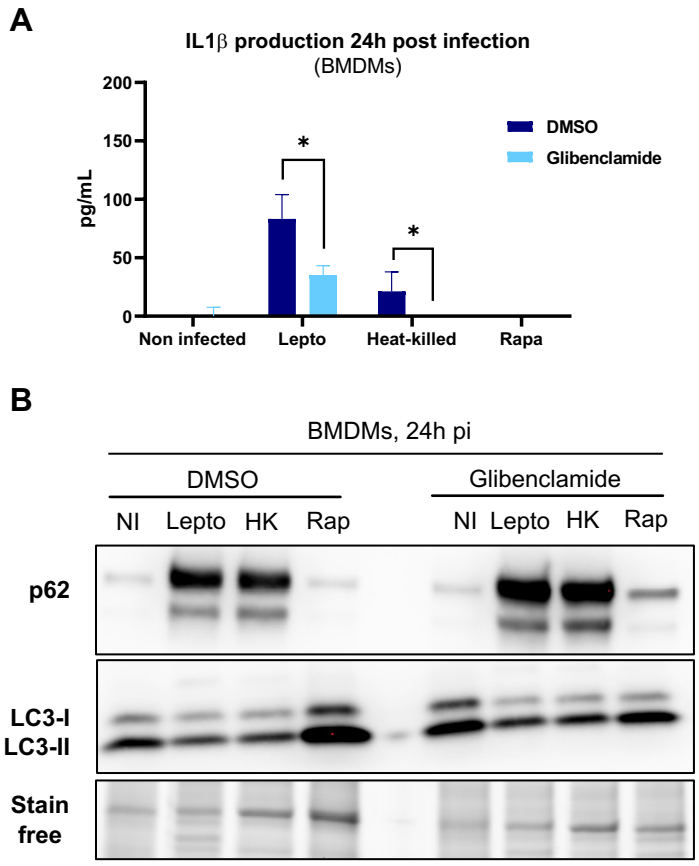

Sup. Figure 3. p62 accumulation induced by leptospires does not rely on NLRP3 inflammasome

A) IL1β dosage by ELISA in BMDMs 24h post-infection with either live or heat-killed (56°C, 30 min) *L. interrogans* serovar Manilae strain L495 at MOI 100 with or without 25 µM glibenclamide (inflammasome inhibitor). Bars correspond to mean +/- SD of technical replicates (n=4). Statistical analyses were performed using Student's t-test with corresponding p values: * for $p < 0.05$. **B)** WB of LC3 and p62 in BMDMs 24h post-infection with either live or heat-killed (56°C, 30 min) *L. interrogans* serovar Manilae strain L495 at MOI 100, or upon autophagy induction with 500 mM rapamycin (Rap) with or without 25 µM glibenclamide.

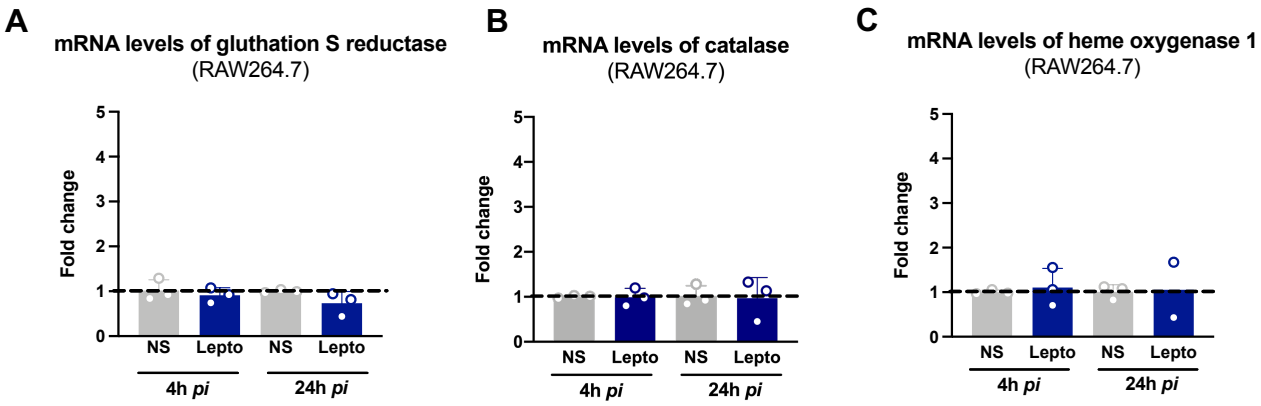

Sup. Figure 4. Infection by leptospires does not trigger transcription of NRF2 antioxidant targets

A-B) RT-qPCR analyses of gluthatione S-reductase, catalase and heme oxygenase 1 mRNA levels in RAW264.7 cells 4h or 24h post-infection with *L. interrogans* serovar Manilae strain L495 at MOI 100. Bars correspond to mean +/- SD of technical replicates (*n*=3).